



OPEN P2X7 receptor antagonism by AZ10606120 significantly reduced in vitro tumour growth in human glioblastoma

Liyen K. Kan¹, Matthew Drill¹, Padmakrishnan C. Jayakrishnan¹, Richard P. Sequeira¹, Emily Galea², Marian Todaro^{1,4,5}, Paul G. Sanfilippo¹, Martin Hunn², David A. Williams³, Terence J. O'Brien^{1,4,5}, Katharine J. Drummond⁶ & Mastura Monif^{1,3,4,5}✉

Glioblastomas are highly aggressive and deadly brain tumours, with a median survival time of 14–18 months post-diagnosis. Current treatment modalities are limited and only modestly increase survival time. Effective therapeutic alternatives are urgently needed. The purinergic P2X7 receptor (P2X7R) is activated within the glioblastoma microenvironment and evidence suggests it contributes to tumour growth. Studies have implicated P2X7R involvement in a range of neoplasms, including glioblastomas, although the roles of P2X7R in the tumour milieu remain unclear. Here, we report a trophic, tumour-promoting role of P2X7R activation in both patient-derived primary glioblastoma cultures and the U251 human glioblastoma cell line, and demonstrate its inhibition reduces tumour growth in vitro. Primary glioblastoma and U251 cell cultures were treated with the specific P2X7R antagonist, AZ10606120 (AZ), for 72 h. The effects of AZ treatment were also compared to cells treated with the current first-line chemotherapeutic drug, temozolomide (TMZ), and a combination of both AZ and TMZ. P2X7R antagonism by AZ significantly depleted glioblastoma cell numbers compared to untreated cells, in both primary glioblastoma and U251 cultures. Notably, AZ treatment was more effective at tumour cell killing than TMZ. No synergistic effect between AZ and TMZ was observed. AZ treatment also significantly increased lactate dehydrogenase release in primary glioblastoma cultures, suggesting AZ-induced cellular cytotoxicity. Our results reveal a trophic role of P2X7R in glioblastoma. Importantly, these data highlight the potential for P2X7R inhibition as a novel and effective alternative therapeutic approach for patients with lethal glioblastomas.

Brain cancer remains notoriously complex and difficult to treat. Gliomas account for approximately 80% of all brain malignancies¹. Of these, a large proportion are glioblastomas, the most infiltrative and aggressive subtype. The median overall survival from glioblastoma diagnosis is estimated at 14–18 months¹, with the 5-year survival rate of under 5%². Disappointedly, survival rates for glioblastoma have not improved over the previous three decades². This is largely due to ongoing limitations in the current treatment options. Despite progress in research on glioblastoma therapeutics, no new and more effective treatments have been translated into clinical care.

The current treatment regime for newly-diagnosed glioblastoma involves an initial maximal safe surgical resection, followed by concomitant radiotherapy and chemotherapy (temozolomide; TMZ) over 6 weeks, and subsequently six additional cycles of maintenance TMZ³. While treatment is multimodal, it serves only a modest prognostic benefit and is often associated with debilitating side-effects^{3–13}. For example, TMZ chemotherapy has been shown to increase survival time by 2.5 months in some patients, with minimal therapeutic benefit in 60–75% of glioblastoma patients^{4–6}. More effective and targeted therapies for gliomas are urgently needed.

A protein of interest in the tumour microenvironment is the P2X7 receptor (P2X7R)¹⁴. P2X7R is a trimeric transmembrane ion channel expressed on haematopoietic cells, including microglia, macrophages, and lymphocytes¹⁵. It binds to ATP and activates at ATP levels exceeding 200 micromolar. P2X7R can distinctly

¹Department of Neuroscience, Central Clinical School, Monash University, Melbourne, VIC, Australia. ²Department of Neurosurgery, The Alfred, Melbourne, VIC, Australia. ³Department of Physiology, The University of Melbourne, Melbourne, VIC, Australia. ⁴Department of Neurology, The Royal Melbourne Hospital, Melbourne, VIC, Australia. ⁵Department of Neurology, The Alfred, Melbourne, VIC, Australia. ⁶Department of Neurosurgery, The Royal Melbourne Hospital, Melbourne, VIC, Australia. ✉email: mastura.monif@monash.edu

transition between two activation states: channel and pore. With transient ATP stimulation, the receptor is a highly selective ion channel that facilitates cationic movement across the plasma membrane. Prolonged exposure to ATP uniquely transforms P2X7R into a non-selective transmembrane pore that is also permeable to aqueous molecules of up to 900 Daltons^{16–18}. The exact role of P2X7R in a physiological setting is unclear, but it is likely associated with cell trophism and cytokine release. Importantly, there are robust associations between P2X7R activation, inflammation, and immune modulation. P2X7R expression and activation has been further implicated in cellular energy metabolism and mitochondrial dysfunction^{19,20}. The roles of P2X7R are likely diverse and its activation might induce either a growth-promoting or cytolytic effect in different pathological contexts.

P2X7R function has been implicated in various cancers, with studies demonstrating receptor involvement in melanoma²¹, uterine epithelial cancer²², leukaemia²³ and lung cancer²⁴. Importantly, in gliomas, P2X7R is expressed on both glioma cells and microglia, the main cellular infiltrates of the glioma microenvironment¹⁴. We have previously demonstrated P2X7R upregulation in gliomas¹⁴. In vitro studies have shown that P2X7R antagonism promoted the growth of glioma cells in the rat C6²⁵ and mouse GL261²⁶ glioma cell lines, suggesting a cytolytic role of P2X7R. In contrast, multiple studies have demonstrated reductions in glioma proliferation following P2X7R antagonism^{27–30}, indicative of trophic P2X7R activity. A further study using rat C6 glioma cells demonstrated increased tumour cell motility following P2X7R stimulation³¹. Previous data from our laboratory on primary patient-derived glioblastoma cultures in vitro revealed a decrease in glioma cell count following P2X7R inhibition with Brilliant Blue G¹⁴. In a pilot study, we further demonstrated a significant reduction in glioblastoma cell numbers in both U251 human glioblastoma cells and primary patient-derived glioblastoma cultures following treatment with 5–25 μM of the specific P2X7R antagonist, AZ10606120 (AZ)³². Despite this, the precise functions of P2X7R in the glioma microenvironment remain unclear.

Here, we expand on our pilot data investigating the effect of P2X7R antagonism in both patient-derived glioblastoma samples and U251 human glioblastoma cells. Additionally, we compare the efficacy of P2X7R antagonism by AZ to that of the conventional chemotherapeutic drug, TMZ.

Results

P2X7R inhibition by AZ depletes tumour cells in a concentration-dependent manner in patient-derived primary glioblastoma samples.

In a previous pilot study, we demonstrated a significant decrease in tumour cell numbers in both U251 cells and primary patient-derived high-grade glioma cultures after treatment with varying doses of AZ for 72 h. We trialled concentrations of 5 and 25 μM for U251 cells and 15 μM for human gliomas, all three of which yielded a significantly lower glioma cell count compared to untreated cells³². Here, we further characterise the effects of AZ-mediated P2X7R antagonism in human glioblastomas. To establish an optimal AZ dosage regimen for treatment of primary patient-derived glioma cultures in vitro, cells at 80% confluency were treated with AZ concentrations of 1, 5, 15, 25, 50 and 100 μM for 72 h. Glial fibrillary acidic protein (GFAP) and DAPI double-positive cells were subsequently quantified for all treatment groups and untreated cells. In all patients, there was a significant reduction in tumour cell number following treatment with 15 μM AZ or greater, compared to untreated cells (mean GFAP + cells = 462.6 ± 102.4), with a mean total GFAP + cell count of 66 ± 23.51 for 15 μM AZ, 23.57 ± 18.19 for 25 μM AZ, 20.86 ± 17.72 for 50 μM AZ, and 21.57 ± 17.78 for 100 μM AZ (Fig. 1). There was no statistically significant difference in GFAP + cell count observed between AZ concentrations of 1 (515 ± 147.4 and 368.9 ± 148.9 cells) and 5 μM (368.9 ± 148.9 cells) versus untreated cells. We selected a dosage of 15 μM of AZ for use in subsequent experiments, given that it was the lowest concentration demonstrating effective tumour cell depletion.

P2X7R inhibition by AZ and its comparison to TMZ chemotherapy.

We have previously demonstrated significant reductions in tumour cell number after treatment with AZ on both U251 human glioblastoma cells and surgically resected human glioma samples³². Extending from these results, our next aim was to elucidate the anti-tumour activity of 15 μM of AZ, in comparison to the most common conventional chemotherapy agent, TMZ. Cells were treated for 72 h with either AZ (15 μM) or TMZ (50 μM). Following treatment, cells were fixed, stained and the number of DAPI + cells for U251 cells, and GFAP + /DAPI + cells for primary glioblastoma cultures were quantified via fluorescence microscopy. We conducted an initial experiment on U251 cells comparing AZ 15 μM to TMZ alone. Both TMZ and AZ depleted U251 cell numbers (2249 ± 77.75 and 1357 ± 56.42 cells, respectively) when compared to untreated cells (2827 ± 127 cells) (Fig. 2A). Interestingly, cells treated with AZ had a significantly lower U251 cell count than TMZ-treated cells (Fig. 2A). Similarly, in a subsequent experiment, treatment with AZ significantly reduced U251 cell count (1309 ± 378.3 cells) compared to both untreated cells (4744 ± 302.4 cells) and TMZ-treated cells (5921 ± 495.1 cells) (Fig. 2B). However, there was no significant tumour inhibition observed with TMZ treatment (Fig. 2B). The effects of AZ and TMZ treatment were also tested at 24 and 48 h post-treatment, but showed no statistically significant difference in tumour cell number compared to untreated cells (Supplementary Fig. 1).

In primary glioblastoma cultures, treatment with 15 μM of AZ also significantly reduced GFAP + cell numbers (114.3 ± 35.9 vs. 569.1 ± 157 cells in AZ and untreated groups, respectively), although there were no significant differences between both the untreated versus TMZ group and the AZ versus TMZ group (Fig. 3A). Of note, there was variability in patient response to TMZ (Fig. 3B), which likely affected the differences in cell count observed between TMZ and treatment groups. Nonetheless, the above data collectively demonstrated a significant reduction in tumour cell count in both U251 cells and human glioblastoma samples following P2X7R antagonism with 15 μM of AZ, supportive of a P2X7R-mediated anti-tumour effect. Additionally, AZ treatment shows potential as either an adjunctive therapy or a more effective treatment alternative to TMZ in U251 cells, although this should be explored further with human glioblastoma samples.

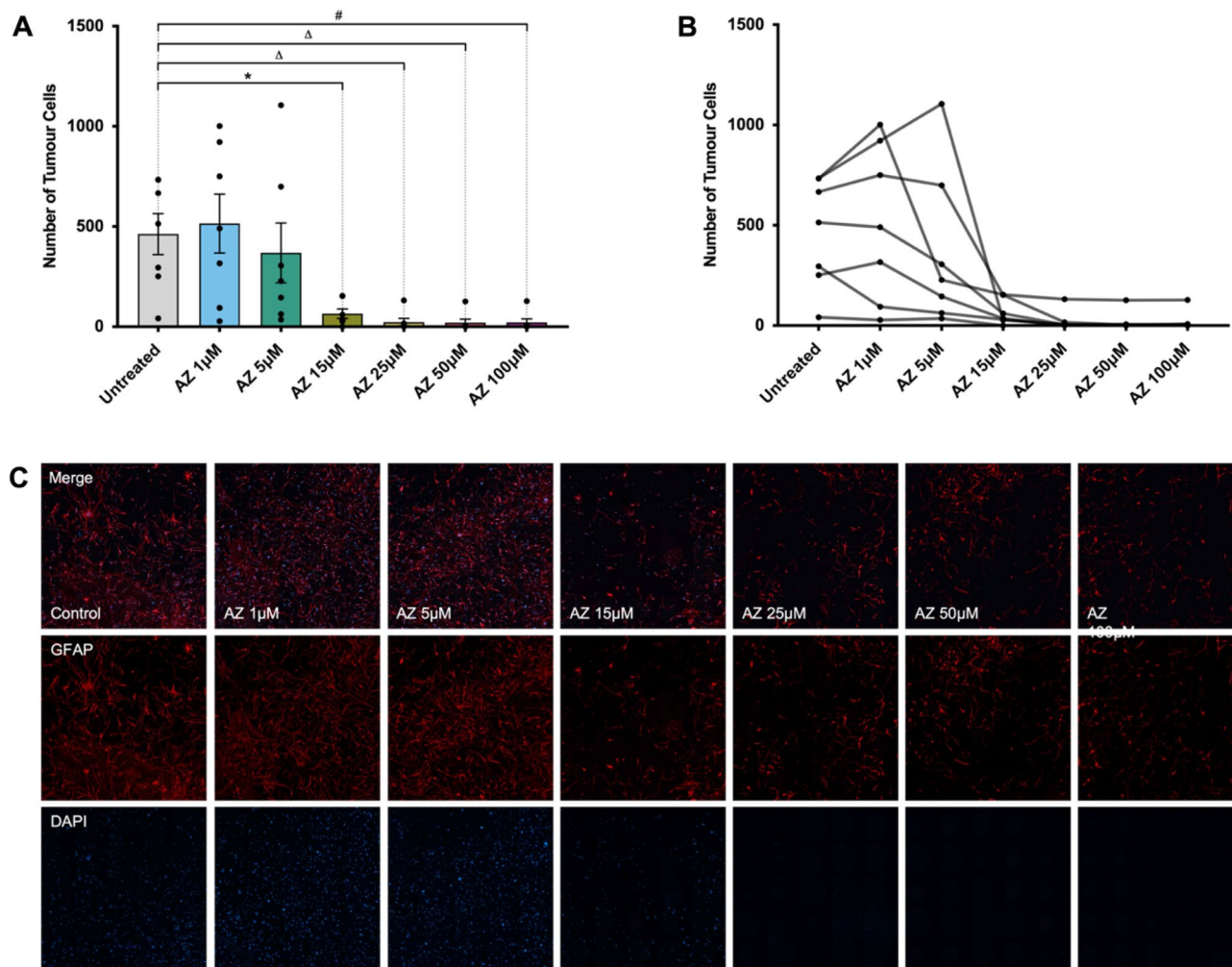


Figure 1. P2X7 receptor (P2X7R) antagonism by AZ10606120 (AZ) across AZ doses of 1–100 μM in human primary glioblastoma cultures. Glioblastoma specimens collected from patients undergoing routine tumour resection surgery were cultured and treated at 80% confluency with 1, 5, 15, 25, 50 or 100 μM of AZ for 72 h. The control group were untreated cells. Cells were fixed and stained with primary rabbit anti-gliial fibrillary acidic protein (GFAP) antibody overnight at 4 °C, followed by secondary goat anti-rabbit antibody conjugated to Texas Red-X for 2 h at room temperature. All cell nuclei were counterstained with DAPI for 1 h at room temperature. Images were acquired with a Nikon Ti-E inverted fluorescence motorised microscope equipped with a sCMOS Andor Zyla camera at 20× objective. The total number of GFAP + /DAPI + cells were quantified across 16 random fields for each sample and treatment group. **(A)** There was significant tumour cell depletion with AZ concentrations of 15 μM or greater. Results were yielded from a one-way repeated measures ANOVA with Tukey's HSD post-hoc, $F(1.61, 9.63) = 9.47$, $p = 0.007$. $N = 7$ patients. Untreated versus AZ 15 μM: mean difference = 396.6 cells, 95% CI = 31.46 to 761.7; Untreated versus AZ 25 μM: mean difference = 439.0 cells, 95% CI = 45.49 to 832.5; Untreated versus AZ 50 μM: mean difference = 441.7 cells, 95% CI = 44.22 to 839.2; Untreated versus AZ 100 μM: mean difference = 441.0 cells, 95% CI = 42.21 to 839.8. * $p = 0.04$, $\Delta p = 0.031$, # $p = 0.032$. Error bars represent SEM. **(B)** Individual patient responses to treatment with 1, 5, 15, 25, 50 and 100 μM AZ. **(C)** Image representation of primary glioblastoma cultures treated with various concentrations of AZ versus untreated control cells. GFAP and DAPI channels are red and blue, respectively.

Co-administration of AZ with TMZ does not synergistically deplete tumour cell number in U251 cells and primary patient-derived glioblastoma cultures. We sought to additionally investigate the effect of AZ and TMZ co-therapy and whether these reagents would synergistically inhibit tumour proliferation. U251 cells were treated with a combination of 15 μM of AZ and 50 μM of TMZ for 72 h. The effect of AZ and TMZ co-therapy was also compared to that of untreated cells, and cells treated with either AZ or TMZ alone. Cells were subsequently fixed, stained and imaged via fluorescence microscopy. DAPI+ and GFAP + /DAPI+ cells were quantified for U251 cells and primary human glioblastoma cultures, respectively. For U251 cells, a one-way ANOVA yielded a statistically significant difference between groups. Notably, there was no significant difference in U251 cell count between cells treated with AZ and TMZ in combination (1326 ± 265 cells) and cells treated with AZ alone (1309 ± 378.3 cells) (Fig. 2B). Both AZ-TMZ co-treated cells and AZ treated cells

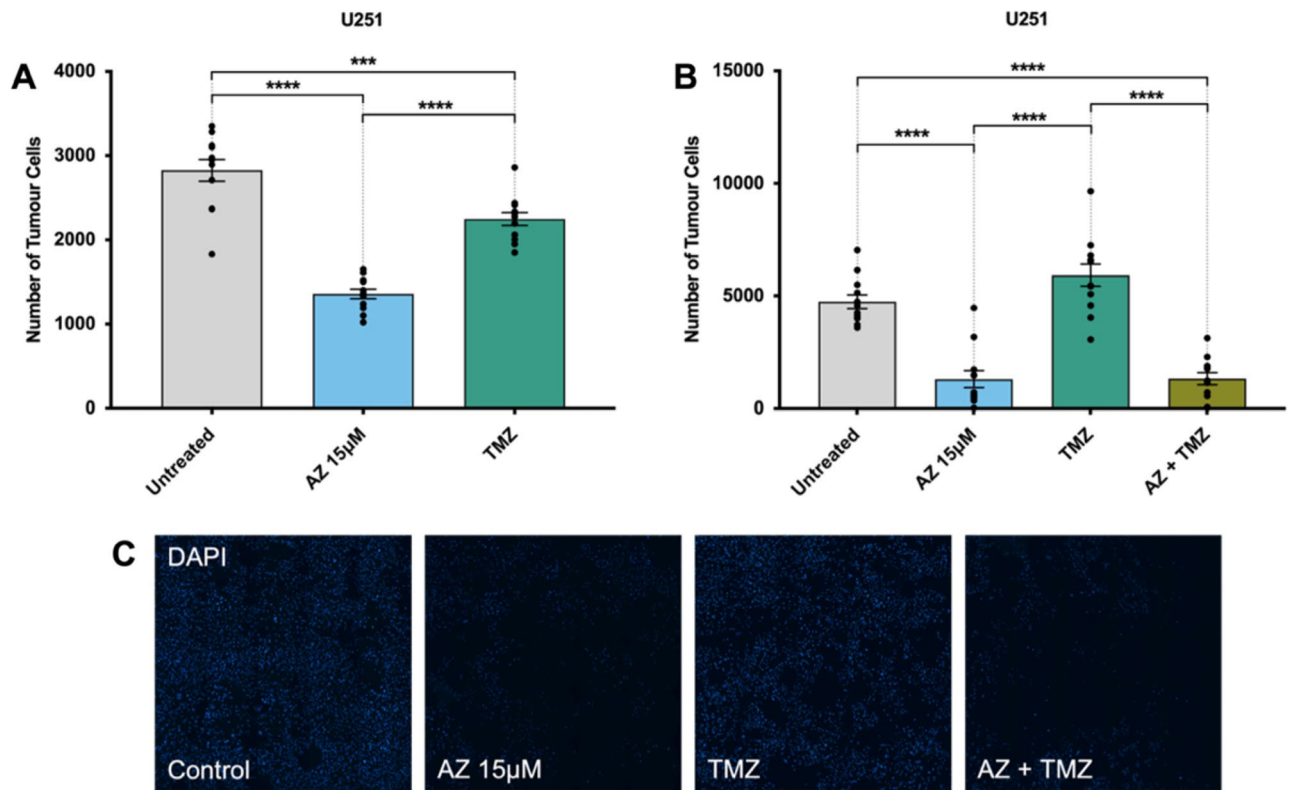


Figure 2. The effects of P2X7 receptor (P2X7R) antagonism by AZ10606120 (AZ) compared to conventional temozolomide (TMZ) chemotherapy on the U251 human glioblastoma cell line. U251 human glioblastoma cells were cultured and treated at 80% confluency with 15 µM AZ, 50 µM TMZ and a combination of AZ + TMZ for 72 h. The control group were untreated cells. U251 cultures were counterstained with DAPI for 1 h at room temperature. Images were acquired with a Nikon Ti-E inverted fluorescence motorised microscope equipped with a sCMOS Andor Zyla camera at 20× objective. The total number of DAPI+ cells were quantified across 16 random fields for each sample and treatment group. **(A)** Comparison of AZ 15 µM with TMZ in U251 cells. Results were yielded from a one-way ANOVA with Tukey's HSD post-hoc, $F(2, 33) = 64.87$, $p < 0.0001$. $N = 12$ replicates. Untreated versus TMZ: mean difference = 578.3 cells, 95% CI = 259.3 to 897.4; Untreated versus AZ 15 µM: mean difference = 1470 cells, 95% CI = 1151 to 1789; AZ 15 µM versus TMZ: mean difference = -891.5, 95% CI = -1211 to -572.5. $***p = 0.0003$, $****p < 0.0001$. Error bars represent SEM. **(B)** Comparison of 15 µM AZ and AZ-TMZ co-therapy with TMZ in U251 cells. Results were yielded from a one-way ANOVA with Tukey's HSD post-hoc. $N = 12$ replicates, $F(3, 44) = 40.77$, $p < 0.0001$. Untreated versus AZ 15 µM: mean difference = 3435 cells, 95% CI = 2035 to 4835; Untreated versus TMZ: mean difference = -1177 cells, 95% CI = -2577 to 223.2, $p = 0.13$; Untreated versus AZ + TMZ: mean difference = 3419 cells, 95% CI = 2019 to 4819; AZ 15 µM versus TMZ: mean difference = -4612 cells, 95% CI = -6012 to -3212. AZ 15 µM versus AZ + TMZ: mean difference = -16.33 cells, 95% CI = -1416 to 1384, $p > 0.99$; TMZ versus AZ + TMZ: mean difference = 4596 cells, 95% CI = 3196 to 5996. $*p < 0.0001$. Error bars represent SEM. **(C)** Image representation of U251 cells treated with 15 µM AZ, TMZ, AZ + TMZ and control.

had significantly lower tumour cell numbers versus untreated cells (4744 ± 302.4 cells) and TMZ-treated cells (5921 ± 495.1 cells) (Fig. 2B).

Similarly, in primary human glioblastoma cultures, there was no significant difference in tumour cell count between AZ-treated (114.3 ± 35.9 cells) and AZ-TMZ co-treated cells (92.42 ± 30.06 cells) (Fig. 3A). Lower tumour cell numbers were observed between both cells treated with AZ and AZ-TMZ, and untreated cells (569.1 ± 157 cells) (Fig. 3A). No statistically significant differences were observed between the AZ and AZ-TMZ groups and TMZ-treated cells, despite the presence of a trend demonstrating increased tumour cell depletion in AZ and AZ-TMZ treated groups.

There was no synergistic anti-tumour effect observed with AZ-TMZ co-administration. We postulated that this result could have been due to the limited bandwidth available for synergistic activity to occur, given that 15 µM of AZ was shown to reduce glioblastoma cell numbers with high efficacy. With low cell numbers in cultures treated with AZ 15 µM, AZ-TMZ combination therapy may not exert a discernible effect; a synergistic effect might hence be observable with lower AZ concentrations. To explore this, we co-treated U251 cells with varying AZ concentrations (1 µM, 5 µM, 15 µM and 25 µM) and TMZ, and compared the effects to both TMZ alone, AZ alone and untreated cells. No statistically significant difference in tumour cell count was detected between U251 cells treated with AZ-TMZ co-therapy and AZ alone, for all AZ concentrations (Fig. 4). However, there was a statistically significant decrease in tumour cell number in AZ-TMZ co-treated cells for both AZ 1 µM (9399 ± 295.8

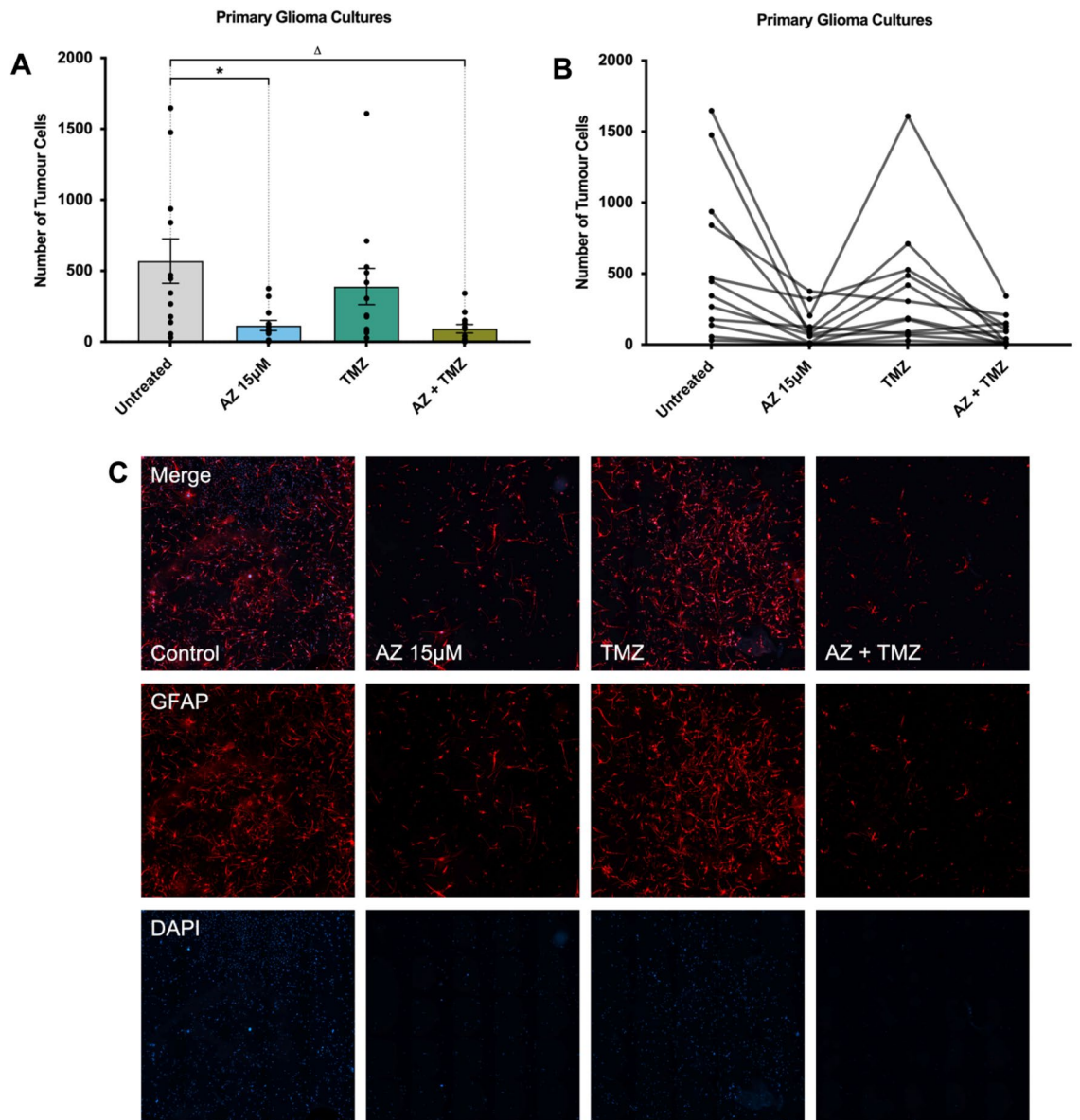


Figure 3. The effects of P2X7 receptor (P2X7R) antagonism by AZ10606120 (AZ) compared to conventional temozolomide (TMZ) chemotherapy on patient-derived primary glioblastoma cultures. Glioblastoma specimens collected from patients undergoing routine tumour resection surgery were cultured and treated at 80% confluency with 15 µM AZ, 50 µM TMZ and a combination of AZ + TMZ for 72 h. The control group were untreated cells. Primary glioblastoma cultures were fixed and stained with primary rabbit anti-gliial fibrillary acidic protein (GFAP) antibody overnight at 4 °C, followed by secondary goat anti-rabbit antibody conjugated to Texas Red-X for 2 h at room temperature. Cells were counterstained with DAPI for 1 h at room temperature. Images were acquired with a Nikon Ti-E inverted fluorescence motorised microscope equipped with a sCMOS Andor Zyla camera at 20× objective. The total number of GFAP + /DAPI + cells were quantified across 16 random fields for each sample and treatment group. **(A)** Comparison of AZ 15 µM and AZ-TMZ co-therapy with TMZ in primary glioblastoma cultures. Results were yielded from a one-way repeated measures ANOVA with Tukey's HSD post-hoc, $F(1.81, 19.9) = 7.79$, $p = 0.004$. $N = 12$ patients. Untreated versus AZ 15 µM: mean difference = 454.8 cells, 95% CI = 13.05 to 896.4, $*p = 0.04$; Untreated versus TMZ: mean difference = 179.3 cells, 95% CI = -182.2 to 540.7, $p = 0.47$; Untreated versus AZ + TMZ: mean difference = 476.7 cells, 95% CI = 69.78 to 883.6, $\Delta p = 0.02$; AZ 15 µM versus TMZ: mean difference = -275.5 cells, 95% CI = -632.5 to 81.46, $p = 0.15$; AZ 15 µM versus AZ + TMZ: mean difference = 21.92 cells, 95% CI = -59.3 to 103.1, $p = 0.85$; TMZ versus AZ + TMZ: mean difference = 297.4 cells, 95% CI = -31.45 to 626.3, $p = 0.08$. Error bars represent SEM. **(B)** Individual patient responses to treatment with AZ 15 µM, TMZ and AZ + TMZ. **(C)** Image representation of primary glioblastoma cultures treated with AZ 15 µM, TMZ, AZ + TMZ and control. GFAP and DAPI channels are red and blue, respectively.

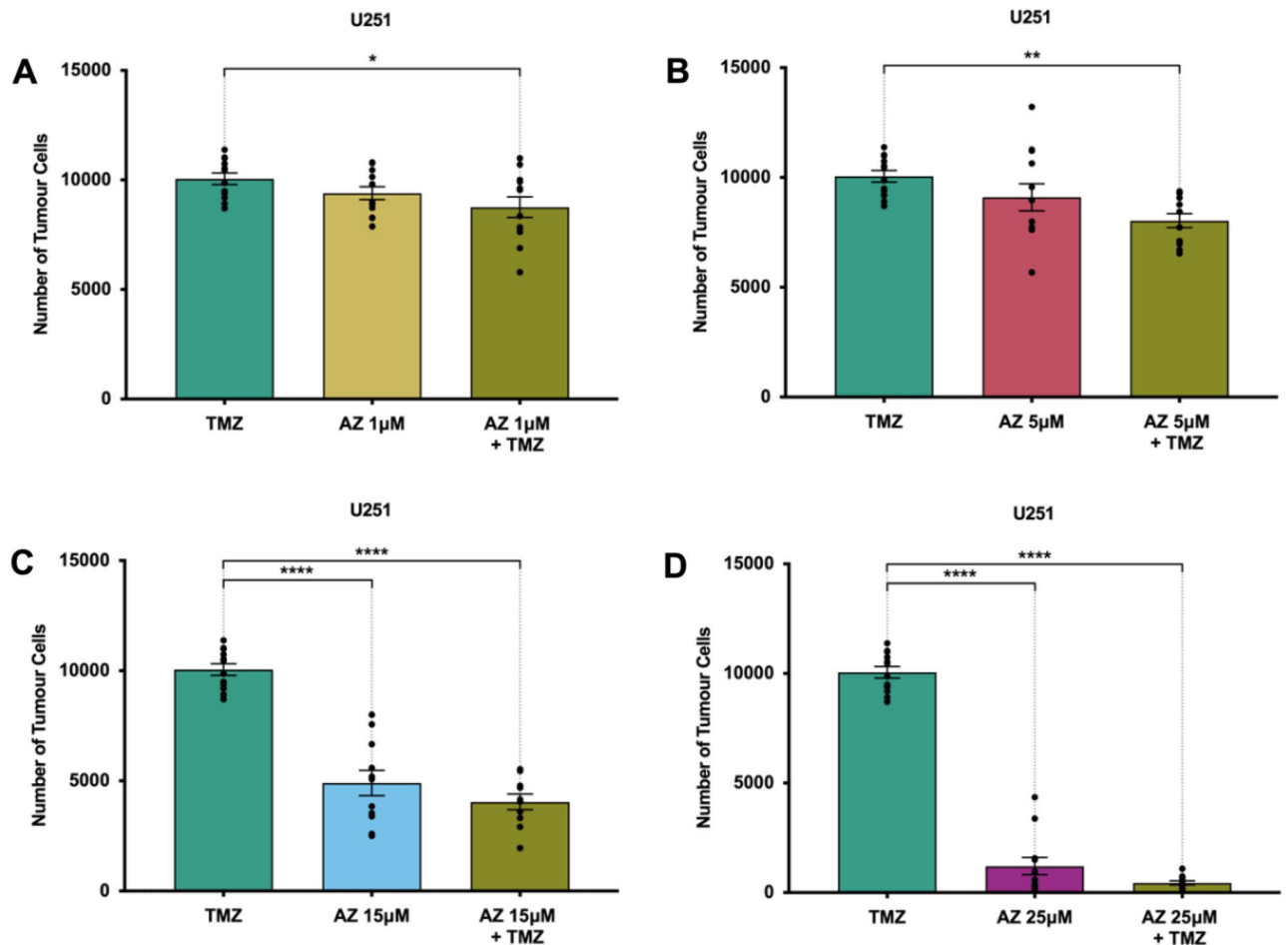


Figure 4. Co-treatment of AZ10606120 (AZ) and temozolomide (TMZ) in U251 cells. U251 human glioblastoma cells were cultured and treated at 80% confluency with various concentrations of AZ, 50 μ M TMZ and a combination of AZ + TMZ for 72 h. Cells were fixed and stained with DAPI for 1 h at room temperature. The total number of DAPI + cells were quantified across 16 random fields for each sample and treatment group. (A) Comparison of AZ, TMZ and AZ + TMZ with AZ 1 μ M in U251 cells. Results were yielded from a one-way ANOVA with Tukey's HSD post-hoc, $F(2, 33) = 3.77$, $p = 0.03$. $N = 12$ replicates. TMZ versus AZ 1 μ M: mean difference = 659.8 cells, 95% CI = -562.5 to 1882, $p = 0.39$; TMZ versus AZ 1 μ M + TMZ: mean difference = 1299 cells, 95% CI = 76.46 to 2521, $*p = 0.04$; AZ 1 μ M versus AZ 1 μ M + TMZ: mean difference = 639 cells, 95% CI = -583.4 to 1861, $p = 0.41$. (B) Comparison of AZ, TMZ and AZ + TMZ with AZ 5 μ M in U251 cells. Results were yielded from a one-way ANOVA with Tukey's HSD post-hoc, $F(2, 33) = 4.05$, $p = 0.03$. $N = 12$ replicates. TMZ versus AZ 5 μ M: mean difference = 958.9 cells, 95% CI = -528.6 to 2446, $p = 0.27$; TMZ versus AZ 5 μ M + TMZ: mean difference = 2024 cells, 95% CI = 536 to 3511, $**p = 0.006$; AZ 5 μ M versus AZ 5 μ M + TMZ: mean difference = 1065 cells, 95% CI = -422.9 to 2552, $p = 0.20$. (C) Comparison of AZ, TMZ and AZ + TMZ with AZ 15 μ M in U251 cells. Results were yielded from a one-way repeated measures ANOVA with Tukey's HSD post-hoc, $F(2, 30) = 3.72$. $N = 12$ patients. TMZ versus AZ 15 μ M: mean difference = 5152 cells, 95% CI = 3728 to 6576; TMZ versus AZ 15 μ M + TMZ: mean difference = 6013 cells, 95% CI = 4552 to 7474; AZ 15 μ M versus AZ 15 μ M + TMZ: mean difference = 860.7 cells, 95% CI = -629.9 to 2351, $p = 0.34$. $****p < 0.0001$. (D) Comparison of AZ, TMZ and AZ + TMZ with AZ 25 μ M in U251 cells. Results were yielded from a one-way repeated measures ANOVA with Tukey's HSD post-hoc, $F(2, 33) = 3.31$, $p = 0.049$. $N = 12$ patients. TMZ versus AZ 25 μ M: mean difference = 8848 cells, 95% CI = 7891 to 9805; TMZ versus AZ 25 μ M + TMZ: mean difference = 9609 cells, 95% CI = 8652 to 10,567; AZ 25 μ M versus AZ 25 μ M + TMZ: mean difference = 761.4 cells, 95% CI = -196.1 to 1719, $p = 0.14$; $****p < 0.0001$. Error bars represent SEM.

cells) and AZ 5 μ M (9100 ± 615 cells) compared to TMZ ($10,059 \pm 262.5$ cells), despite no significant changes in cell count between AZ alone and TMZ (Fig. 4A, B). Given that there was no observed difference in U251 cell count between AZ and AZ-TMZ treated groups, this data is not supportive of AZ-TMZ mediated synergy. However, this requires further clarification. Nonetheless, our results demonstrate improved tumour-depleting activity by AZ over TMZ, with no synergistic anti-tumour effect observed between AZ and TMZ.

AZ increases lactate dehydrogenase (LDH) release in human tumour samples. Treatment with AZ resulted in significantly lower glioblastoma cell counts. To determine whether this anti-tumour effect was

due to plasma membrane damage, we conducted a lactate-dehydrogenase (LDH) cytotoxicity assay to assess the LDH levels present in primary glioblastoma culture supernatants. Glioblastoma cultures were treated at 80% confluency with 1 μM , 5 μM , 15 μM , 25 μM , 50 μM or 100 μM of AZ for 72 h. LDH levels in culture supernatants were subsequently quantified and are directly proportional to absorbance levels at 492 nm. Notably, there was a significantly higher level of LDH in the culture supernatants of cells treated with 15 μM of AZ onwards, compared to the untreated control (Fig. 5). There was also a trend for increasing supernatant LDH levels with increasing AZ concentration. Treatment with TMZ did not induce LDH release in patient-derived glioblastoma cultures (Fig. 5). From this data, AZ treatment likely induces a cytotoxic membrane-damaging effect variable to TMZ, although the exact mode of cell death requires further investigation.

Discussion

Glioblastomas are highly invasive and serve as the third leading cause of cancer-related death in young people aged 15 to 24. Importantly, despite advances in treatment, no improvement in glioma survival rates have been observed across the past three decades². Here, we investigated the effect of P2X7R antagonism by AZ in both human U251 glioblastoma cells—which are devoid of immune cells—and primary patient-derived glioblastoma cultures. Importantly, treatment with AZ for 72 h significantly depleted tumour cells in vitro, in both primary patient-derived glioblastoma cultures and U251 glioblastoma cells. AZ treatment was also more effective than conventional TMZ chemotherapy, although no synergistic anti-tumour effect was observed between AZ and TMZ. LDH levels were significantly increased following AZ treatment, indicative of cellular cytotoxicity, but more clarification of the mode of tumour cell death induced by AZ treatment is required. Nonetheless, this study highlights the potential for P2X7R inhibition to serve as a novel therapeutic for glioblastoma, superior to conventional TMZ.

An earlier study conducted by our laboratory was one of the first to trial the effects of AZ treatment in U251 cells and human glioma samples³². This dataset only included a dosage of 5 and 25 μM of AZ for U251 cells and 15 μM for human glioma samples. A dose–response experiment of AZ in U251 cells was subsequently conducted by our laboratory and established a half maximal inhibitory (IC₅₀) concentration of 17 μM (Drill et al. Unpublished data). In this study, we sought to establish the lowest effective treatment concentration of AZ in primary human glioblastoma cultures for use in subsequent cell quantification and cytotoxicity experiments. Across a 72-h treatment period, we observed a significant reduction in tumour cell numbers in tumours treated with 15 μM of AZ and above (Fig. 1). There was also a trend for increasing tumour inhibition with increasing doses of AZ (Fig. 1). A concentration of 15 μM was the lowest effective AZ dosage for human glioblastoma samples.

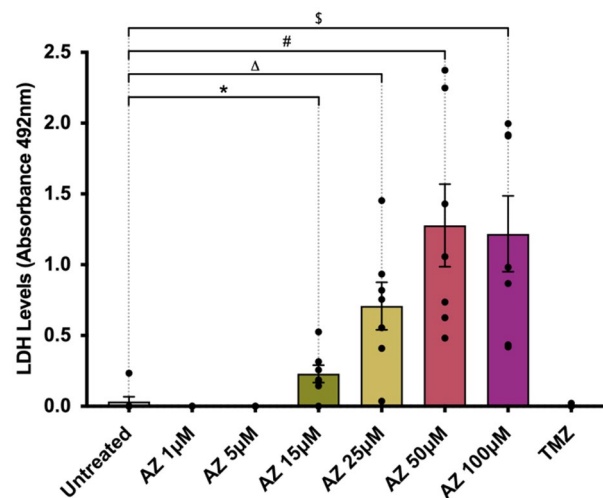


Figure 5. Lactate dehydrogenase (LDH) levels in human primary glioblastoma cultures following P2X7 receptor (P2X7R) antagonism with AZ10606120 (AZ). Glioblastoma specimens collected from patients undergoing routine tumour resection surgery were cultured and treated at 80% confluency with 1, 5, 15, 25, 50 or 100 μM of AZ for 72 h. As a comparison, cells were also treated with 50 μM of temozolomide (TMZ), the conventional chemotherapeutic drug. The control group were untreated cells. Culture supernatants were processed and utilised in an LDH cytotoxicity assay. Supernatant LDH levels are proportional to the absorbance at 492 nm. Treatment with AZ concentrations of 15 μM or greater significantly increased LDH release by primary human glioblastoma cells. Results were yielded from a one-way repeated measures ANOVA with Dunnett's post-hoc, $F(1.48, 8.87) = 16.93$, $p = 0.002$. $N = 7$ patients. Untreated versus AZ 1 μM : mean difference = 0.03, 95% CI = -0.09 to 0.15, $p = 0.84$; Untreated versus AZ 5 μM : mean difference = 0.03, 95% CI = -0.09 to 0.15, $p = 0.84$; Untreated versus AZ 15 μM : mean difference = -0.20, 95% CI = -0.34 to -0.05, $*p = 0.01$; Untreated versus AZ 25 μM : mean difference = -0.68, 95% CI = -1.26 to -0.09, $\Delta p = 0.03$; Untreated versus AZ 50 μM : mean difference = -1.25, 95% CI = -2.28 to -0.21, $\#p = 0.02$; Untreated versus AZ 100 μM : mean difference = -1.18, 95% CI = -2.09 to -0.28, $\$p = 0.015$; Untreated versus TMZ: mean difference = 0.03, 95% CI = -0.09 to 0.15, $p = 0.90$. Error bars represent SEM.

AZ dosage in the current literature is variable, with previous studies using concentrations equivalent to 0.3 μM ³³, 10 μM ³⁴, 100 μM or 200 μM ³⁵. However, these studies were conducted on models of mammary and pancreatic cancer^{33–35}, and not glioma.

Importantly, treatment with 15 μM of AZ at 72 h significantly depleted tumour cell numbers in both U251 cells and human glioblastoma samples (Fig. 2, Supplementary Fig. 1). In U251 cells, there were significantly lower numbers of tumour cells in cultures treated with AZ, compared to those treated with TMZ, across two experiments (Fig. 2). However, in patient glioblastoma cultures, no significant changes in tumour cell numbers were observed between the same groups, although an overall trend for higher efficacy of AZ over TMZ was speculated (Fig. 3A). There was notable variability in patient response to TMZ, which might have affected the overall statistical differences observed between the two groups (Fig. 3B). Variability in patient response to TMZ therapy is well-documented. While the drug generally increases overall survival by 2.5 months⁴, around 60–75% of glioblastoma patients receive no therapeutic benefit due to genetic or acquired TMZ resistance^{5,6,36}. In this study, specimens were collected from both newly diagnosed and recurrent glioblastoma patients, so it is not surprising that TMZ resistance was observed in some samples. Of note, O6-methylguanine methyltransferase (MGMT) promoter methylation status, commonly linked to differential responses to TMZ³⁷, was not established in this study. There was also evidence of acquired TMZ resistance in U251 cells. Initially, there was a minor anti-tumour effect with TMZ administration (Fig. 2A), which diminished in a subsequent experiment with later U251 passages (Fig. 2B). While the U251 cell line is known to be sensitive to TMZ³⁷, there is documentation of acquired TMZ resistance in U251 cells likely due to mismatch repair deficiency³⁸. We observed no statistically significant tumour-killing activity with AZ treatment after 24 or 48 h (Supplementary Fig. 1). There is likely a time-dependent effect of AZ, influenced by factors including threshold cellular AZ concentration and differential sensitivity to AZ at various cell-cycle stages. Nonetheless, in this study all U251 cells and patients appeared to have responded well to AZ treatment after 72 h (Figs. 2, 3). Indeed, the anti-tumour effect of AZ has been implicated in other neoplastic diseases, but limited studies have elucidated its role in glioblastomas. In a neuroblastoma mouse model, P2X7R inhibition with AZ resulted in a significant reduction in VEGF secretion, subsequently hindering blood vessel formation required for angiogenesis³⁹. AZ treatment also inhibited tumour cell migration and invasion and reduced the fibrous stroma in pancreatic cancer⁴⁰. AZ administration further inhibited mesothelioma growth in both in vitro and in vivo experiments⁴¹. Previous work from our laboratory revealed increased expression of granulocyte-macrophage colony-stimulating factor (GM-CSF) in U251 cells following treatment with AZ⁴². In glioblastomas, GM-CSF promotes immunosuppression by favouring a shift toward granulocytic cells, rather than lymphocytic lineages, during haematopoiesis⁴³. GM-CSF upregulation also induces overexpression of IL-4 receptor- α on myeloid-derived suppressor cells, which facilitates immunosuppression⁴⁴. Few other studies have investigated the effects of P2X7R inhibition by AZ in human gliomas. The results of this current study support a trophic role of P2X7R in glioblastoma, where its inhibition by AZ exerts a largely anti-tumour effect.

We also wanted to determine whether co-treatment with AZ and TMZ fosters a synergistic anti-tumour response. No synergistic effect was observed with AZ-TMZ co-administration at AZ concentrations of 1 μM , 5 μM , 15 μM and 25 μM in U251 cells (Fig. 2B, 4). We initially assessed for AZ-TMZ synergy with 15 μM of AZ but postulated that the lack of effect could have been due to the massive tumour-depleting activity of AZ 15 μM , limiting the bandwidth for an observable synergistic effect of both drugs to occur. However, given that no significantly enhanced reductions in tumour cell numbers were observed between U251 cultures treated with AZ (1 and 5 μM) and AZ-TMZ co-therapy, it is likely that both drugs do not act in synergy. It is possible that the TMZ concentration of 50 μM was not sufficient to induce an anti-tumour effect, and thus the reductions in cell count in groups treated with AZ and TMZ were solely due to AZ activity. TMZ dosages for in vitro studies have been controversial. The current standard of care incorporates maintenance TMZ at a dose of 150–200 mg/m² on days 1 to 5 of a 28-day cycle⁶, with peak concentrations of the drug reaching 30–50 μM in tumour and plasma⁴⁵. We selected the TMZ dosage based on this data. However, within the literature, there are discrepancies with determining optimal clinically relevant dosages. For example, other studies have suggested optimal TMZ doses of 0.82–9.94 μM ⁴⁶, 1.55–4.64 μM ⁴⁷ and 14.94–34.51 μM ⁴⁸, based on peak drug concentrations in either tumour, peri-tumour or cerebrospinal fluid. Treatment length might have further affected TMZ efficacy, although multiple studies have utilised the 72-h timeframe with observed efficacy^{49–52}. It is important to note that this is not representative of the clinical TMZ treatment regimen, which involves cyclic, long-term TMZ use; a single high dose of TMZ is likely to have diminished efficacy over continued usage³⁶. Clinically relevant drug doses are difficult to replicate in in vitro experiments, which serves as a major limitation of this study. Nonetheless, here, TMZ was ineffective in reducing tumour growth in primary glioblastoma cultures and did not act in synergy with various concentrations of AZ.

Tumour inhibition by P2X7R antagonism is likely governed by a multitude of downstream mediators. Our data support a tumour depleting role of AZ treatment, but it is currently unclear how the compound exerts its anti-tumour activity. As a first step, we explored whether AZ was causing cytotoxicity via plasma membrane damage, through the release of LDH in patient samples. LDH is a ubiquitous cytoplasmic enzyme secreted into the extracellular space upon plasma membrane damage. Its release into cell culture supernatants has been widely utilised as a measure of cellular damage, particularly of cells undergoing apoptosis and necrosis⁵³. We observed a significant increase in supernatant LDH levels following treatment with AZ at 15 μM onwards, with a trend showing increasing LDH release with increasing AZ dosage (Fig. 5). In contrast, TMZ did not promote LDH release in patient glioblastoma samples. P2X7R blockade by AZ has been weakly linked to LDH release, although studies are limited and present conflicting results. For example, in immortalised malignant pleural mesothelioma cell lines, receptor antagonism by AZ increased LDH release⁴⁰, whereas pre-treatment with AZ prevented the ATP-mediated release of LDH in the J774 macrophage cell line⁵⁴. The latter study also observed P2X7-mediated IL-1 β release in LPS-stimulated macrophages, which was associated with a small amount of LDH release⁵⁴.

Nonetheless, in the present study, the trend displaying increasing LDH release coupled with decreasing tumour cell numbers with increasing AZ dosage is suggestive of AZ-mediated cytotoxicity.

The mechanisms of tumour inhibition by P2X7R are likely multifaceted, involving crosstalk between glioblastoma cells, immune mediators and other components of the tumour microenvironment. P2X7R blockade likely hinders NLRP3 inflammasome-controlled release of tumour-promoting mediators such as IL-1 β . For example, since the P2X7R pore mediates IL-1 β release⁵⁵, inhibiting receptor activity is likely to greatly diminish IL-1 β levels within the tumour microenvironment leading to reduced overall immunosuppression. IL-1 β is known to fuel microglial polarisation into a trophic, immunosuppressive phenotype ideal for glioma growth^{55,56}. The cytokine also directly acts on glioma cells by increasing tumour cell migration and invasion⁵⁷. Moreover, halting P2X7R activity might induce metabolic dysfunction of tumour cells directly, leading to tumour cell death and hence glioma inhibition. P2X7R has been shown to increase cellular lactate output and glycogen storage, as well as upregulate glycolytic enzymes, enhancing the ability of tumour cells to adapt to unfavourable ambient conditions⁵⁸. Enhanced mitochondrial depolarisation has also been observed in C6 glioma cells following P2X7R activation⁵⁹. There seems to be a clear metabolic association with P2X7R stimulation. Interestingly, receptor stimulation has been shown to assist in the maintenance of cancer stem cells^{60,61}, which are key contributors to treatment resistance and tumour recurrence⁶². Hence, P2X7R antagonism might also enhance tumour killing by preventing cancer stem cell development. Investigating the efficacy of AZ treatment in glioblastoma stem cells—particularly three-dimensional glioblastoma cell culture systems⁶³—would be pivotal, given that an ideal therapeutic would also be effective against cells that are resistant to conventional treatment.

Collectively, these experiments suggest a basal cancer-promoting role of P2X7R activation in the glioblastoma setting. P2X7R antagonism by AZ inhibits tumourigenesis with high efficacy. The downstream tumour-inhibiting mechanisms of P2X7R blockade by AZ are still unclear, but results from this study support cytotoxic P2X7R-mediated anti-tumour activity facilitated by glioblastoma cells alone (evidenced by U251 cells), in addition to potential downstream immunological responses within the wider tumour microenvironment (evidenced by primary human glioblastoma cultures). There was no synergistic anti-tumour effect with AZ-TMZ combination therapy. However, AZ treatment appeared to be more effective than conventional TMZ chemotherapy. The next stage is to illuminate potential downstream responses of P2X7R inhibition, particularly in terms of immunological and metabolic mediators. Delineating associations between P2X7R expression and various pro-tumour, anti-tumour, and microenvironmental components would be a valuable first step. Furthermore, repeating these experiments on glioblastoma cancer stem cells is necessary to test the efficacy of AZ in the context of treatment resistance and tumour recurrence. Nonetheless, P2X7R inhibition significantly depleted glioblastoma cells in U251 cells and patient glioblastoma samples. This potentiates P2X7R as an ideal new therapeutic target for aggressive brain cancer. Importantly, AZ shows promise as an alternative or adjunctive therapy for glioblastoma.

Materials and methods

Patient-derived primary glioblastoma culture. Human glioblastoma samples were collected from patients undergoing routine tumour resection surgery by a qualified neurosurgeon at The Royal Melbourne Hospital and The Alfred, as part of the Alfred Brain Tumour Biobank (Melbourne, Australia). Protocols for obtaining and handling human brain tissue were reviewed and approved by the Human Research Ethics Committees (HREC) of the RMH (HREC 2006.119) and The Alfred (HREC 2017.450). All experiments were performed in accordance with relevant guidelines and regulations. Written informed consent was obtained from all patients or respective legally authorised representatives. Upon resection, tumour samples were fragmented and immersed in Earle's Balanced Salt Solution (EBSS; Thermo Fisher Scientific Australia, cat no. 14155063) containing papain (200 units; Merck Australia, cat no. P3125) at 37 °C for 35 min. Digested tissue samples were then washed in triplicate with culture media—Minimum Essential Medium (MEM; Thermo Fisher Scientific Australia, cat no. 10370021) supplemented with 1 mM D-glucose (Merck Australia, cat no. G7021), 2 mM L-glutamine (Merck Australia, cat no. G7513), 50 units/mL penicillin–streptomycin (Thermo Fisher Scientific Australia, cat no. 15070063), 10% heat inactivated foetal bovine serum (FBS; Thermo Fisher Scientific Australia, cat no. 10100147) and Corning® MITO + Serum Extender (Merck Australia, cat no. DLW355006). Cells were homogenised and seeded at approximately 1×10^5 cells per well into 12-well cell culture plates (Merck Australia, cat no. SIAL0512) containing 18 mm round glass coverslips (Thermo Fisher Scientific Australia). Coverslips were pre-coated with poly-D-lysine hydrobromide (PDL; Merck Australia, cat no. P6407). Primary glioblastoma cultures were maintained in a humidified incubator at 37 °C with 5% CO₂.

U251 glioblastoma cell culture. The U-251 MG (U251) human glioblastoma cell line was obtained from Merck Australia (cat no. 09063001, RRID: CVCL_0021). U251 cells were cultured in Dulbecco's Modified Eagle's Medium (DMEM; Lonza, cat no. 12-604F) supplemented with 1 mM sodium pyruvate (Thermo Fisher Scientific Australia, cat no. 11360070), 50 units/mL penicillin–streptomycin, 10% FBS and 1% non-essential amino acids (NEAA; Thermo Fisher Scientific Australia, cat no. 11140050). Cells were maintained in a humidified incubator at 37 °C with 5% CO₂ and passaged routinely at 80% confluency.

Treatment reagents. Primary human glioblastoma cultures and U251 cultures were treated at 80% confluency with the P2X7R antagonist, AZ106061206 (AZ; Tocris Biosciences, cat no. 3323), and/or the conventional chemotherapy drug, temozolomide (TMZ; Merck Australia, cat no. T2577), for 72 h. To compare the effects of various treatment lengths, U251 cells were also treated with AZ and/or TMZ for 24 h and 48 h. Both AZ and TMZ were dissolved in dimethyl sulfoxide (DMSO; Merck Australia, cat no. W387509) prior to use according to manufacturers' instructions. A TMZ concentration of 50 μ M was utilised for all experiments involving TMZ treatment, based on previous studies demonstrating peak physiological TMZ concentrations of 30–50 μ M in

both tumour and plasma of patients undergoing TMZ maintenance therapy for glioblastoma⁴⁵. The following concentrations of AZ were used: 1 μ M, 5 μ M, 15 μ M, 25 μ M, 50 μ M and 100 μ M.

Cell staining. Following treatment, primary human glioblastoma cultures and U251 cultures were fixed in a solution of 1:1 acetone-methanol for 15 min at -20°C . For primary glioblastoma cultures, cells were pre-incubated with primary rabbit anti-glial fibrillary acidic protein (GFAP) antibody (Dako, cat no. Z0334, RRID: AB_10013382) diluted 1:400 in Phosphate Buffered Saline (PBS; Thermo Fisher Scientific Australia, cat no. 14190144) overnight at 4°C , followed by secondary goat anti-rabbit antibody conjugated to Texas Red-X (Thermo Fisher Scientific Australia, cat no. T-862, RRID: AB_2556781) diluted 1:200 in PBS for 2 h at room temperature. Cell nuclei were subsequently stained with 5 μ M of DAPI (Thermo Fisher Scientific Australia, cat no. D1306) for 1 h at room temperature. Cells were washed in triplicate with PBS after each staining step and mounted on glass slides with Dako fluorescence mounting medium (Dako, cat no. S3023). For U251 cells, cell nuclei were stained with DAPI for 1 h at room temperature and subsequently mounted.

Tumour cell quantification. Cells were imaged with a Nikon Ti-E inverted motorised fluorescence microscope with a sCMOS Andor Zyla camera at $20\times$ objective (Monash Micro Imaging – Alfred Research Alliance, Melbourne, Australia). For each sample/passage and treatment group, the total number of viable tumour cells – GFAP+/DAPI+ and DAPI+ cells for patient glioblastoma cultures and U251 cells, respectively – were quantified over 16 random fields. All images were analysed using the ImageJ image processing software (version 2.9.0/1.53t)⁶⁴.

Lactate dehydrogenase (LDH) cytotoxicity assay. Lactate dehydrogenase (LDH) levels in primary glioblastoma culture supernatants were quantified using the Roche colorimetric LDH Cytotoxicity Detection Kit (Roche, cat no. 11644793001), as per manufacturer's instructions. Briefly, cell-free supernatants were incubated with LDH reaction mixture at a 1:1 ratio for 25 min at room temperature. Absorbance was measured at 492 nm using the FLUOstar[®] Omega Plate Reader (BMG LABTECH). Absorbance was directly proportional to supernatant LDH levels.

Statistical analysis. All statistical analyses were conducted using the Graphpad Prism software (version 9). Normality of datasets was assessed via Q–Q plots. A one-way repeated measures ANOVA or one-way ANOVA with Brown-Forsythe and Welch corrections was utilised for experiments on patient samples and U251 cells, respectively. Post-hoc analyses included the Tukey's HSD and Dunnett's multiple comparisons tests. Data were expressed as mean \pm SEM. An alpha level of 0.05 was set as the significance level. The mean difference and corresponding 95% confidence interval (CI) were reported where necessary.

Data availability

The data supporting the findings of this study are available from the corresponding author, Dr Mastura Monif, upon request.

Received: 1 December 2022; Accepted: 22 May 2023

Published online: 24 May 2023

References

- Hanif, F., Muzaffar, K., Perveen, K., Malhi, S. M. & Simjee, S. U. Glioblastoma multiforme: A review of its epidemiology and pathogenesis through clinical presentation and treatment. *Asian Pacific J. Cancer Prev. APJCP* **18**, 3–9 (2017).
- Tamimi, A. F. & Juweid, M. in *Glioblastoma* (ed S. De Vleeschouwer) (Codon Publications Copyright: The Authors., 2017).
- Tan, A. C. *et al.* Management of glioblastoma: State of the art and future directions. *CA Cancer J. Clin.* **70**(4), 299–312. <https://doi.org/10.3322/caac.21613> (2020).
- Stupp, R. *et al.* Effects of radiotherapy with concomitant and adjuvant temozolomide versus radiotherapy alone on survival in glioblastoma in a randomised phase III study: 5-year analysis of the EORTC-NCIC trial. *Lancet Oncol.* **10**, 459–466. [https://doi.org/10.1016/s1470-2045\(09\)70025-7](https://doi.org/10.1016/s1470-2045(09)70025-7) (2009).
- Chamberlain, M. C. Temozolomide: Therapeutic limitations in the treatment of adult high-grade gliomas. *Expert Rev. Neurother.* **10**, 1537–1544. <https://doi.org/10.1586/ern.10.32> (2010).
- Stupp, R. *et al.* Radiotherapy plus concomitant and adjuvant temozolomide for glioblastoma. *N. Engl. J. Med.* **352**(10), 987–996. <https://doi.org/10.1056/NEJMoa043330> (2005).
- Klein, M. *et al.* Effect of radiotherapy and other treatment-related factors on mid-term to long-term cognitive sequelae in low-grade gliomas: A comparative study. *Lancet* **360**, 1361–1368 (2002).
- Pendergrass, J. C., Targum, S. D. & Harrison, J. E. Cognitive impairment associated with cancer: A brief review. *Innov. Clin. Neurosci.* **15**, 36–44 (2018).
- Han, X., Xue, X., Zhou, H. & Zhang, G. A molecular view of the radioresistance of gliomas. *Oncotarget* **8**, 100931–100941. <https://doi.org/10.18632/oncotarget.21753> (2017).
- Johnson, D. R. & Chang, S. M. In *Glioma: Immunotherapeutic Approaches* (ed. Yamanaka, R.) 26–40 (Springer, New York, 2012).
- Marumoto, T. & Saya, H. Molecular biology of glioma. *Adv. Exp. Med. Biol.* **746**, 2–11. https://doi.org/10.1007/978-1-4614-3146-6_1 (2012).
- Lara-Velazquez, M. *et al.* Advances in brain tumor surgery for glioblastoma in adults. *Brain Sci.* **7**, 166. <https://doi.org/10.3390/brainsci7120166> (2017).
- Oliver, L. *et al.* Drug resistance in glioblastoma: Are persisters the key to therapy?. *Cancer Drug Resist.* **3**, 287–301. <https://doi.org/10.20517/cdr.2020.29> (2020).
- Monif, M. *et al.* P2X7 receptors are a potential novel target for anti-glioma therapies. *J. Inflamm.* **11**, 25. <https://doi.org/10.1186/s12950-014-0025-4> (2014).
- Volonte, C., Apolloni, S., Skaper, S. D. & Burnstock, G. P2X7 receptors: Channels, pores and more. *CNS Neurol. Disord. Drug Targets* **11**, 705–721 (2012).

16. Di Virgilio, F., Dal Ben, D., Sarti, A. C., Giuliani, A. L. & Falzoni, S. The P2X7 receptor in infection and inflammation. *Immunity* **47**, 15–31. <https://doi.org/10.1016/j.immuni.2017.06.020> (2017).
17. Adinolfi, E. *et al.* Basal activation of the P2X7(7) ATP receptor elevates mitochondrial calcium and potential, increases cellular ATP levels, and promotes serum-independent growth. *Mol. Biol. Cell* **16**, 3260–3272. <https://doi.org/10.1091/mbc.E04-11-1025> (2005).
18. Franceschini, A. *et al.* The P2X7 receptor directly interacts with the NLRP3 inflammasome scaffold protein. *Faseb J.* **29**, 2450–2461. <https://doi.org/10.1096/fj.14-268714> (2015).
19. Sarti, A. C. *et al.* Mitochondrial P2X7 receptor localization modulates energy metabolism enhancing physical performance. *Function* <https://doi.org/10.1093/function/zqab005> (2021).
20. Wilkaniec, A. *et al.* P2X7 receptor is involved in mitochondrial dysfunction induced by extracellular alpha synuclein in neuroblastoma SH-SY5Y cells. *Int. J. Mol. Sci.* **21**(11), 3959. <https://doi.org/10.3390/ijms21113959> (2020).
21. White, N., Butler, P. E. & Burnstock, G. Human melanomas express functional P2X(7) receptors. *Cell Tissue Res.* **321**, 411–418 (2005).
22. Li, X., Zhou, L., Feng, Y. H., Abdul-Karim, F. W. & Gorodeski, G. I. The P2X7 receptor: A novel biomarker of uterine epithelial cancers. *Cancer Epidemiol. Biomarkers Prev.* **15**, 1906–1913 (2006).
23. Zhang, X. *et al.* The role of P2X7 receptor in ATP-mediated human leukemia cell death: Calcium influx-independent. *Acta Biochim. Biophys. Sin. (Shanghai)* **41**, 362–369 (2009).
24. Boldrini, L. *et al.* P2X7 protein expression and polymorphism in non-small cell lung cancer (NSCLC). *J. Negat. Results Biomed.* **13**, 16. <https://doi.org/10.1186/1477-5751-13-16> (2014).
25. Fang, J. *et al.* P2X7R suppression promotes glioma growth through epidermal growth factor receptor signal pathway. *Int. J. Biochem. Cell Biol.* **45**, 1109–1120. <https://doi.org/10.1016/j.biocel.2013.03.005> (2013).
26. Tamajusuku, A. S. *et al.* Characterization of ATP-induced cell death in the GL261 mouse glioma. *J. Cell Biochem.* **109**, 983–991. <https://doi.org/10.1002/jcb.22478> (2010).
27. Ryu, J. K., Jantarantotai, N., Serrano-Perez, M. C., McGeer, P. L. & McLarnon, J. G. Block of purinergic P2X7R inhibits tumor growth in a C6 glioma brain tumor animal model. *J. Neuropathol. Exp. Neurol.* **70**, 13–22. <https://doi.org/10.1097/NEN.0b013e318201d4d4> (2011).
28. Fang, K. M. *et al.* Expression of macrophage inflammatory protein-1alpha and monocyte chemoattractant protein-1 in glioma-infiltrating microglia: Involvement of ATP and P2X7 receptor. *J. Neurosci. Res.* **89**, 199–211. <https://doi.org/10.1002/jnr.22538> (2011).
29. Bergamin, L. S. *et al.* Involvement of purinergic system in the release of cytokines by macrophages exposed to glioma-conditioned medium. *J. Cell Biochem.* **116**, 721–729. <https://doi.org/10.1002/jcb.25018> (2015).
30. Ji, Z. *et al.* Involvement of P2X7 receptor in proliferation and migration of human glioma cells. *Biomed. Res. Int.* **2018**, 8591397. <https://doi.org/10.1155/2018/8591397> (2018).
31. Wei, W., Ryu, J. K., Choi, H. B. & McLarnon, J. G. Expression and function of the P2X(7) receptor in rat C6 glioma cells. *Cancer Lett.* **260**, 79–87 (2008).
32. Kan, L. K. *et al.* P2X7 receptor antagonism inhibits tumour growth in human high-grade gliomas. *Purinergic Signal* **16**, 327–336. <https://doi.org/10.1007/s11302-020-09705-2> (2020).
33. Brisson, L. *et al.* P2X7 receptor promotes mouse mammary cancer cell invasiveness and tumour progression, and is a target for anticancer treatment. *Cancers* **12**(9), 2342. <https://doi.org/10.3390/cancers12092342> (2020).
34. Giannuzzo, A. *et al.* Targeting of the P2X7 receptor in pancreatic cancer and stellate cells. *Int. J. Cancer* **139**, 2540–2552. <https://doi.org/10.1002/ijc.30380> (2016).
35. Mohammed, A. *et al.* Lack of chemopreventive effects of P2X7R inhibitors against pancreatic cancer. *Oncotarget* **8**, 97822–97834. <https://doi.org/10.18632/oncotarget.22085> (2017).
36. Arora, A. & Somasundaram, K. Glioblastoma versus temozolomide: Can the red queen race be won?. *Cancer Biol. Ther.* **20**, 1083–1090. <https://doi.org/10.1080/15384047.2019.1599662> (2019).
37. Lee, S. Y. Temozolomide resistance in glioblastoma multiforme. *Genes Dis.* **3**, 198–210. <https://doi.org/10.1016/j.gendis.2016.04.007> (2016).
38. Stritzelberger, J., Distel, L., Buslei, R., Fietkau, R. & Putz, F. Acquired temozolomide resistance in human glioblastoma cell line U251 is caused by mismatch repair deficiency and can be overcome by lomustine. *Clin. Transl. Oncol.* **20**, 508–516. <https://doi.org/10.1007/s12094-017-1743-x> (2018).
39. Amoroso, F. *et al.* The P2X7 receptor is a key modulator of the PI3K/GSK3beta/VEGF signaling network: Evidence in experimental neuroblastoma. *Oncogene* **34**, 5240–5251. <https://doi.org/10.1038/ncr.2014.444> (2015).
40. Rotondo, J. C. *et al.* The role of purinergic P2X7 receptor in inflammation and cancer: Novel molecular insights and clinical applications. *Cancers* **14**(5), 1116. <https://doi.org/10.3390/cancers14051116> (2022).
41. Amoroso, F. *et al.* P2X7 targeting inhibits growth of human mesothelioma. *Oncotarget* **7**, 49664–49676. <https://doi.org/10.18632/oncotarget.10430> (2016).
42. Drill, M. *et al.* Inhibition of purinergic P2X receptor 7 (P2X7R) decreases granulocyte-macrophage colony-stimulating factor (GM-CSF) expression in U251 glioblastoma cells. *Sci. Rep.* **10**, 14844. <https://doi.org/10.1038/s41598-020-71887-x> (2020).
43. Kast, R. E. *et al.* Glioblastoma-synthesized G-CSF and GM-CSF contribute to growth and immunosuppression: Potential therapeutic benefit from dapsone, fenofibrate, and ribavirin. *Tumour Biol.* **39**, 1010428317699797. <https://doi.org/10.1177/1010428317699797> (2017).
44. Kohanbash, G. *et al.* GM-CSF promotes the immunosuppressive activity of glioma-infiltrating myeloid cells through interleukin-4 receptor- α . *Cancer Res.* **73**, 6413–6423. <https://doi.org/10.1158/0008-5472.Can-12-4124> (2013).
45. Beier, D. *et al.* Efficacy of clinically relevant temozolomide dosing schemes in glioblastoma cancer stem cell lines. *J. Neurooncol.* **109**, 45–52. <https://doi.org/10.1007/s11060-012-0878-4> (2012).
46. Rosso, L. *et al.* A new model for prediction of drug distribution in tumor and normal tissues: Pharmacokinetics of temozolomide in glioma patients. *Cancer Res.* **69**, 120–127. <https://doi.org/10.1158/0008-5472.Can-08-2356> (2009).
47. Quinn, J. A. *et al.* Phase II trial of temozolomide plus o6-benzylguanine in adults with recurrent, temozolomide-resistant malignant glioma. *J. Clin. Oncol.* **27**, 1262–1267. <https://doi.org/10.1200/jco.2008.18.8417> (2009).
48. Brada, M. *et al.* Phase I dose-escalation and pharmacokinetic study of temozolomide (SCH 52365) for refractory or relapsing malignancies. *Br. J. Cancer* **81**, 1022–1030. <https://doi.org/10.1038/sj.bjc.6690802> (1999).
49. Zhu, Y. *et al.* Characterization of temozolomide resistance using a novel acquired resistance model in glioblastoma cell lines. *Cancers* **14**(9), 2211. <https://doi.org/10.3390/cancers14092211> (2022).
50. Perazzoli, G. *et al.* Temozolomide resistance in glioblastoma cell lines: Implication of MGMT, MMR, P-glycoprotein and CD133 expression. *PLoS One* **10**, e0140131. <https://doi.org/10.1371/journal.pone.0140131> (2015).
51. Soni, V. *et al.* In vitro and in vivo enhancement of temozolomide effect in human glioblastoma by non-invasive application of cold atmospheric plasma. *Cancers* **13**(17), 4485. <https://doi.org/10.3390/cancers13174485> (2021).
52. Le Calvé, B. *et al.* Long-term in vitro treatment of human glioblastoma cells with temozolomide increases resistance in vivo through up-regulation of GLUT transporter and aldo-keto reductase enzyme AKR1C expression. *Neoplasia* **12**(9), 727–739. <https://doi.org/10.1593/neo.10526> (2010).
53. Kumar, P., Nagarajan, A. & Uchil, P. D. Analysis of cell viability by the lactate dehydrogenase assay. *Cold Spring Harb. Protoc.* <https://doi.org/10.1101/pdb.prot095497> (2018).

54. Sluyter, R. & Vine, K. L. N-alkyl-substituted isatins enhance P2X7 receptor-induced interleukin-1 β release from murine macrophages. *Med. Inflamm.* **2016**, 2097219. <https://doi.org/10.1155/2016/2097219> (2016).
55. Monif, M. *et al.* Interleukin-1beta has trophic effects in microglia and its release is mediated by P2X7R pore. *J. Neuroinflamm.* **13**, 173. <https://doi.org/10.1186/s12974-016-0621-8> (2016).
56. Monif, M., Reid, C. A., Powell, K. L., Smart, M. L. & Williams, D. A. The P2X7 receptor drives microglial activation and proliferation: A trophic role for P2X7R pore. *J. Neurosci.* **29**, 3781–3791. <https://doi.org/10.1523/JNEUROSCI.5512-08.2009> (2009).
57. Fathima Hurmath, K., Ramaswamy, P. & Nandakumar, D. N. IL-1 β microenvironment promotes proliferation, migration, and invasion of human glioma cells: Proliferation, migration, invasion by IL-1 β . *Cell Biol. Int.* **38**(12), 1415–1422. <https://doi.org/10.1002/cbin.10353> (2014).
58. Amoroso, F., Falzoni, S., Adinolfi, E., Ferrari, D. & Di Virgilio, F. The P2X7 receptor is a key modulator of aerobic glycolysis. *Cell Death Dis.* **3**, e370. <https://doi.org/10.1038/cddis.2012.105> (2012).
59. Matysiński, D. *et al.* P2X7 receptor: The regulator of glioma tumor development and survival. *Purinerg. Signal* **18**, 135–154. <https://doi.org/10.1007/s11302-021-09834-2> (2022).
60. Arnaud-Sampaio, V. F., Rabelo, I. L. A., Ulrich, H. & Lameu, C. The P2X7 receptor in the maintenance of cancer stem cells, chemoresistance and metastasis. *Stem Cell Rev. Rep.* **16**, 288–300. <https://doi.org/10.1007/s12015-019-09936-w> (2020).
61. Chiozzi, P. *et al.* Amyloid β -dependent mitochondrial toxicity in mouse microglia requires P2X7 receptor expression and is prevented by nimodipine. *Sci. Rep.* **9**, 6475. <https://doi.org/10.1038/s41598-019-42931-2> (2019).
62. Phi, L. T. H. *et al.* Cancer stem cells (CSCs) in drug resistance and their therapeutic implications in cancer treatment. *Stem Cells Int.* **2018**, 5416923. <https://doi.org/10.1155/2018/5416923> (2018).
63. Zanon, M. *et al.* Irradiation causes senescence, ATP release, and P2X7 receptor isoform switch in glioblastoma. *Cell Death Dis.* <https://doi.org/10.1038/s41419-022-04526-0> (2022).
64. Schneider, C. A., Rasband, W. S. & Eliceiri, K. W. NIH Image to ImageJ: 25 years of image analysis. *Nat. Methods* **9**, 671–675. <https://doi.org/10.1038/nmeth.2089> (2012).

Acknowledgements

This research was made possible by the generous donations of brain tumour tissue from patients and their families at both The Royal Melbourne Hospital and The Alfred. We would also like to thank all neurosurgeons, nurses, pathologists and theatre staff at The Royal Melbourne Hospital and The Alfred for assisting with the specimen collection process.

Author contributions

L.K.K.: specimen collection, conducted all experimental work and data analysis, drafting and write-up of entire manuscript; M.D.: assisted with specimen collection and experimental work; P.C.J.: conducted experimental work; R.P.S.: conducted experimental work; E.G.: facilitated specimen collection and patient consenting; M.T.: assisted with specimen collection and biobanking; P.S.: assisted with statistical data analysis; M.H.: conducted surgical resection of specimens, provided research oversight and intellectual input, drafting of manuscript; D.A.W.: provided research oversight and intellectual input, drafting of manuscript; T.J.O.: assisted with overall project design, research oversight and intellectual input, drafting of manuscript; K.J.D.: conducted surgical resection of specimens, provided research oversight and intellectual input, drafting of manuscript; M.M.: designed the overall study and provided intellectual and experimental input, drafting of manuscript.

Funding

This research was funded by an Australian Government Research Training Program Scholarship and the National Health and Medical Research Council (NHMRC) Ideas Grant.

Competing interests

The authors declare no competing interests.

Additional information

Supplementary Information The online version contains supplementary material available at <https://doi.org/10.1038/s41598-023-35712-5>.

Correspondence and requests for materials should be addressed to M.M.

Reprints and permissions information is available at www.nature.com/reprints.

Publisher's note Springer Nature remains neutral with regard to jurisdictional claims in published maps and institutional affiliations.



Open Access This article is licensed under a Creative Commons Attribution 4.0 International License, which permits use, sharing, adaptation, distribution and reproduction in any medium or format, as long as you give appropriate credit to the original author(s) and the source, provide a link to the Creative Commons licence, and indicate if changes were made. The images or other third party material in this article are included in the article's Creative Commons licence, unless indicated otherwise in a credit line to the material. If material is not included in the article's Creative Commons licence and your intended use is not permitted by statutory regulation or exceeds the permitted use, you will need to obtain permission directly from the copyright holder. To view a copy of this licence, visit <http://creativecommons.org/licenses/by/4.0/>.

© The Author(s) 2023